Targetting of the gene encoding fibrillin-1 recapitulates the vascular aspect of Marfan syndrome

Lygia Pereira[1,2], Konstantinos Andrikopoulos[1,3], Jenny Tian[1], Sui Ying Lee[1], Douglas R. Keene[4], Robert Ono[4], Dieter P. Reinhardt[4], Lynn Y. Sakai[4], Nancy Jensen Biery[5], Tracie Bunton[6], Harry C. Dietz[5,7] & Francesco Ramirez[1]

Aortic aneurysm and dissection account for about 2% of all deaths in industrialized countries; they are also components of several genetic diseases, including Marfan syndrome (MFS)[1]. The vascular phenotype of MFS results from mutations in fibrillin-1 (*FBN1*), the major constituent of extracellular microfibrils[2,3]. Microfibrils, either associated with or devoid of elastin, give rise to a variety of extracellular networks in elastic and non-elastic tissues[3]. It is believed that microfibrils regulate elastic fibre formation by guiding tropo-elastin deposition during embryogenesis and early post-natal life[4]. Hence, vascular disease in MFS is thought to result when *FBN1* mutations preclude elastic fibre maturation by disrupting microfibrillar assembly. Here we report a gene-targetting experiment in mice that indicates that fibrillin-1 microfibrils are predominantly engaged in tissue homeostasis rather than elastic matrix assembly. This finding, in turn, suggests that aortic dilation is due primarily to the failure by the microfibrillar array of the adventitia to sustain physiological haemodynamic stress, and that disruption of the elastic network of the media is a secondary event.

The strategy to target the murine gene encoding fibrillin-1 (*Fbn1*) was designed to replicate the dominant-negative effect of fibrillin-1 mutations in MFS[2]. Because interstitial in-frame deletions account for approximately 10% of MFS mutations[2], we replaced 6 kb of *Fbn1* encompassing exons 19–24 (ref. 5) with a neomycin-resistance (*neo*) expression cassette (Fig. 1*a*). Loss of these exons was predicted to yield a centrally deleted monomer missing 272 residues. The deletion overlaps a region of the mouse gene whose human counterpart has been associated with mutations causing a particularly severe MFS phenotype[6,7]. Southern analysis of DNA from 192 transfected embryonic stem cell clones[8] identified three correctly targetted clonal colonies (Fig. 1*b*). Cells from one line (*mg*Δ) were injected into blastocysts and produced a chimaeric mouse that, after mating with a C57BL/6J female, transmitted the mutation to the next generation (Fig. 1*b*). The *mg*Δ embryonic stem-cell line was differentiated *in vitro*[8] and used to purify RNA for RT-PCR analysis.

Sequencing the amplified products confirmed the in-frame deletion of exons 19–24 in transcripts derived from the targetted allele; identical results were later obtained with RNA samples from homozygous mutant mice (data not shown). Quantitative RT-PCR showed about a tenfold reduction in steady-state fibrillin-1 mRNA levels in the lungs, skin and skeletal muscles of two randomly chosen *mg*Δ/*mg*Δ mice (Fig. 1*e*). The same decrease was seen in northern and slot-blot hybridizations of RNA purified from the skin of homozygous mutant mice (Fig. 1*c*,*d*). There was no change in the relative accumulation of fibrillin-2 mRNA between mutant and control samples—excluding a compensatory effect by this structurally related gene product (data not shown)[9]. Reduced mRNA expression from the mutant *Fbn1* allele is probably due to transcriptional interference by the *neo* cassette[10,11]. Homozygous *mg*Δ mice were therefore expected to produce only small amounts of mutant fibrillin-1. Immunoprecipitation of metabolically labelled polypeptides from cultured fibroblasts of homozygous mutant and wild-type mice confirmed the presence of shortened fibrillin-1 in the former compared to the latter samples (Fig. 2*a*). Western blotting results were consistent with the above-mentioned estimates of mutant mRNA levels (data not shown).

Immunohistochemical analysis of *mg*Δ/*mg*Δ tissues documented a substantial reduction of extracellular fibrillin-1, but normal elastin staining (Fig. 2*b*). This was true even in tissues in which expression of fibrillin-1 predates and vastly exceeds that of fibrillin-2 (ref. 12) and in which fibrillin-1 microfibrils were believed to guide elastic fibre formation, such as the elastic tunica of large muscle arteries[4,13]. Immunohistochemical comparison of extracellular fibrillin-1 deposition by cultured dermal fibroblasts from *mg*Δ/*mg*Δ mice and control littermates revealed both quantitative and qualitative differences (Fig. 3). In contrast to the elaborate network of immunoreactive fibrillin-1 fibrils seen in control lines, mutant cultures showed only scant amounts of immunoreactive material 72 hours after plating. Mutant cells had the ability to accumulate extracellular fibrillin-1 over time; however, the architecture of immunoreactive material at 120 hours remained primitive when compared to the multi-layered meshwork of wild-type cultures (Fig. 3). Electron microscopy demonstrated only a few microfibrillar aggregates in long-term (about 2 months) mutant cultures compared to wild-type cells (data not shown). Immunoelectron microscopy confirmed the *in vitro* finding by documenting the presence of microfibrils, as well as normal elastic fibres, in the skin of both wild-type and homozygous mutant mice (Fig. 2*c*). These results are remarkably similar to those observed in MFS tissues, in which seemingly normal microfibrils are shown by electron microscopy despite severely reduced microfibrillar immunostaining[14]. Taken together, the data suggest that mutant fibrillin-1 monomers can polymerize, and that elastic fibres can assemble in the absence of normal fibrillin-1 macro-aggregates.

Consistent with the dominant-negative pathogenic model for MFS[2], heterozygous *mg*Δ/+ mice that express very low levels of mutant product are morphologically and histologically indistinguishable from wild-type littermates, live a normal lifespan and are fertile. There is also no fetal loss of *mg*Δ/*mg*Δ mice, nor do they exhibit gross phenotypic abnormalities at birth. However,

[1]*Brookdale Center for Developmental and Molecular Biology, Mount Sinai School of Medicine, One Gustave L. Levy Place, New York, New York 10029, USA.* [2]*Istituto de Biociencias, Departamento de Biologia, University of São Paulo, São Paulo, SP 05508, Brazil.* [3]*Cutaneous Biology Research Center, Massachusetts General Hospital, Harvard Medical School, Boston, Massachusetts 02129, USA.* [4]*Shriners Hospital for Children, Portland, Oregon 97201, USA.* [5]*Departments of Pediatrics, Medicine and Molecular Biology and Genetics,* [6]*Department of Comparative Medicine and Pathology and* [7]*Howard Huges Medical Institute, Johns Hopkins University School of Medicine, Baltimore, Maryland 21205, USA. Correspondence should be addressed to F.R. e-mail: ramirez@msvax.mssm.edu*

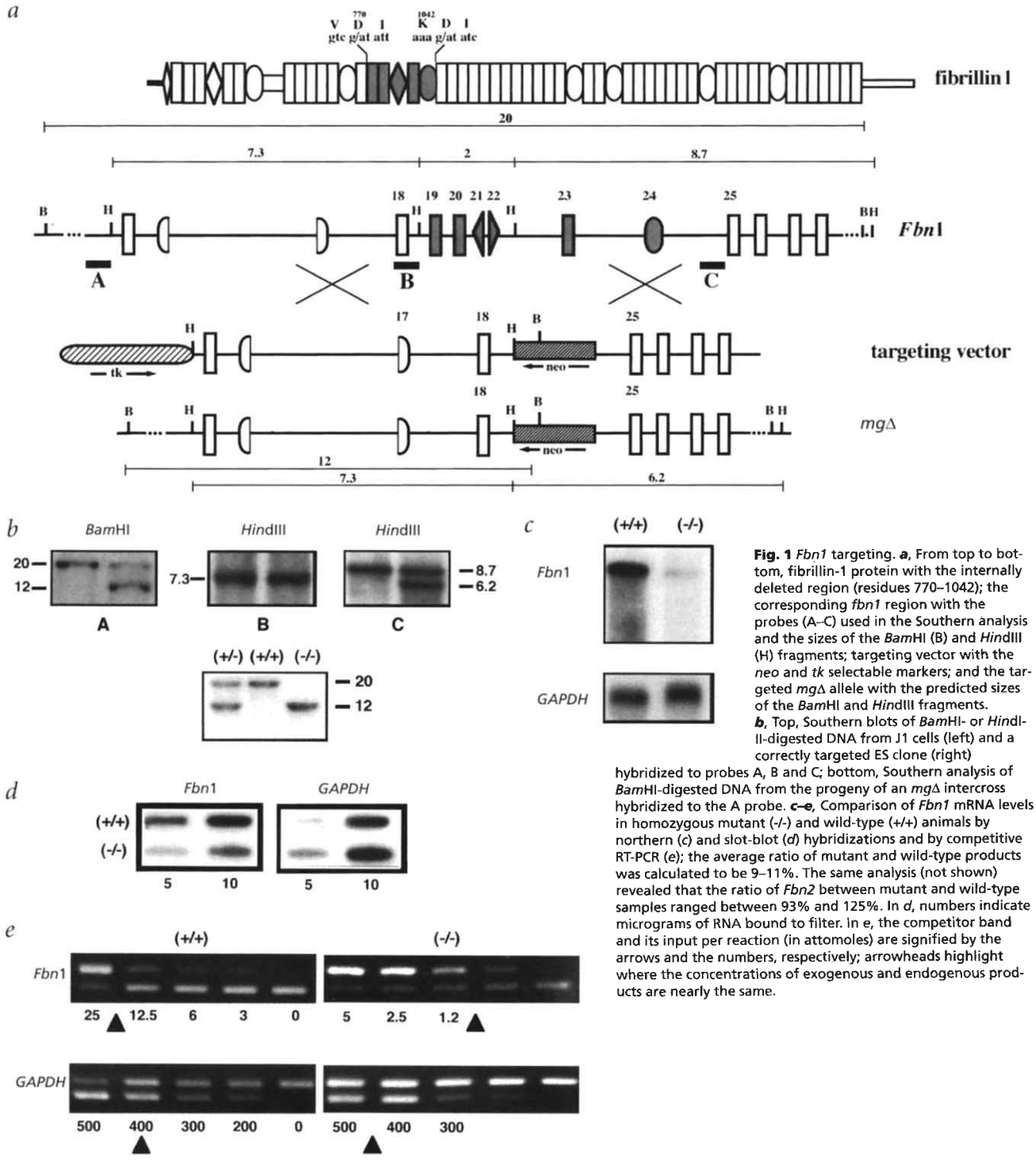

Fig. 1 *Fbn1* targeting. ***a***, From top to bottom, fibrillin-1 protein with the internally deleted region (residues 770–1042); the corresponding *fbn1* region with the probes (A–C) used in the Southern analysis and the sizes of the *Bam*HI (B) and *Hin*dIII (H) fragments; targeting vector with the *neo* and *tk* selectable markers; and the targeted *mg*Δ allele with the predicted sizes of the *Bam*HI and *Hin*dIII fragments. ***b***, Top, Southern blots of *Bam*HI- or *Hin*dIII-digested DNA from J1 cells (left) and a correctly targeted ES clone (right) hybridized to probes A, B and C; bottom, Southern analysis of *Bam*HI-digested DNA from the progeny of an *mg*Δ intercross hybridized to the A probe. ***c–e***, Comparison of *Fbn1* mRNA levels in homozygous mutant (*-/-*) and wild-type (*+/+*) animals by northern (*c*) and slot-blot (*d*) hybridizations and by competitive RT-PCR (*e*); the average ratio of mutant and wild-type products was calculated to be 9–11%. The same analysis (not shown) revealed that the ratio of *Fbn2* between mutant and wild-type samples ranged between 93% and 125%. In *d*, numbers indicate micrograms of RNA bound to filter. In *e*, the competitor band and its input per reaction (in attomoles) are signified by the arrows and the numbers, respectively; arrowheads highlight where the concentrations of exogenous and endogenous products are nearly the same.

they all die suddenly of cardiovascular complications before reaching weaning age (approximately three weeks after birth). Necropsy was performed on nine homozygous mutant animals that had died naturally between nine and eighteen days of age. All showed evidence of vascular compromise with documented haemothorax, haemopericardium or pulmonary haemorrhage. Six animals showed significant thinning of the wall of the proximal ascending aorta, suggesting aneurysmal dilatation. Associated findings included focal fragmentation of elastic fibres, accumulation of amorphous matrix and dissection of blood into the aortic media (Fig. 4). More-chronic lesions showed expansion of the intramural thrombus, recruitment of inflammatory cells, and an adventitial reaction of cellular proliferation when the full thickness of the wall was breached (Fig. 4). Although pathology was generally confined to the aortic root, invasion of a more distal segment was documented in one animal. The abundance and architecture of the elastic fibres appeared preserved between focal lesions and in unaffected tissues. Pulmonary vessels occasionally appeared distended and hyalinized, but their appearance upon elastin staining was not appreciably different from that in heterozygous or homozygous wild-type animals. Multifocal distention and coalescence of alveoli suggesting emphysema were occasionally observed in *mg*Δ/*mg*Δ mice. No skeletal manifestations were noted.

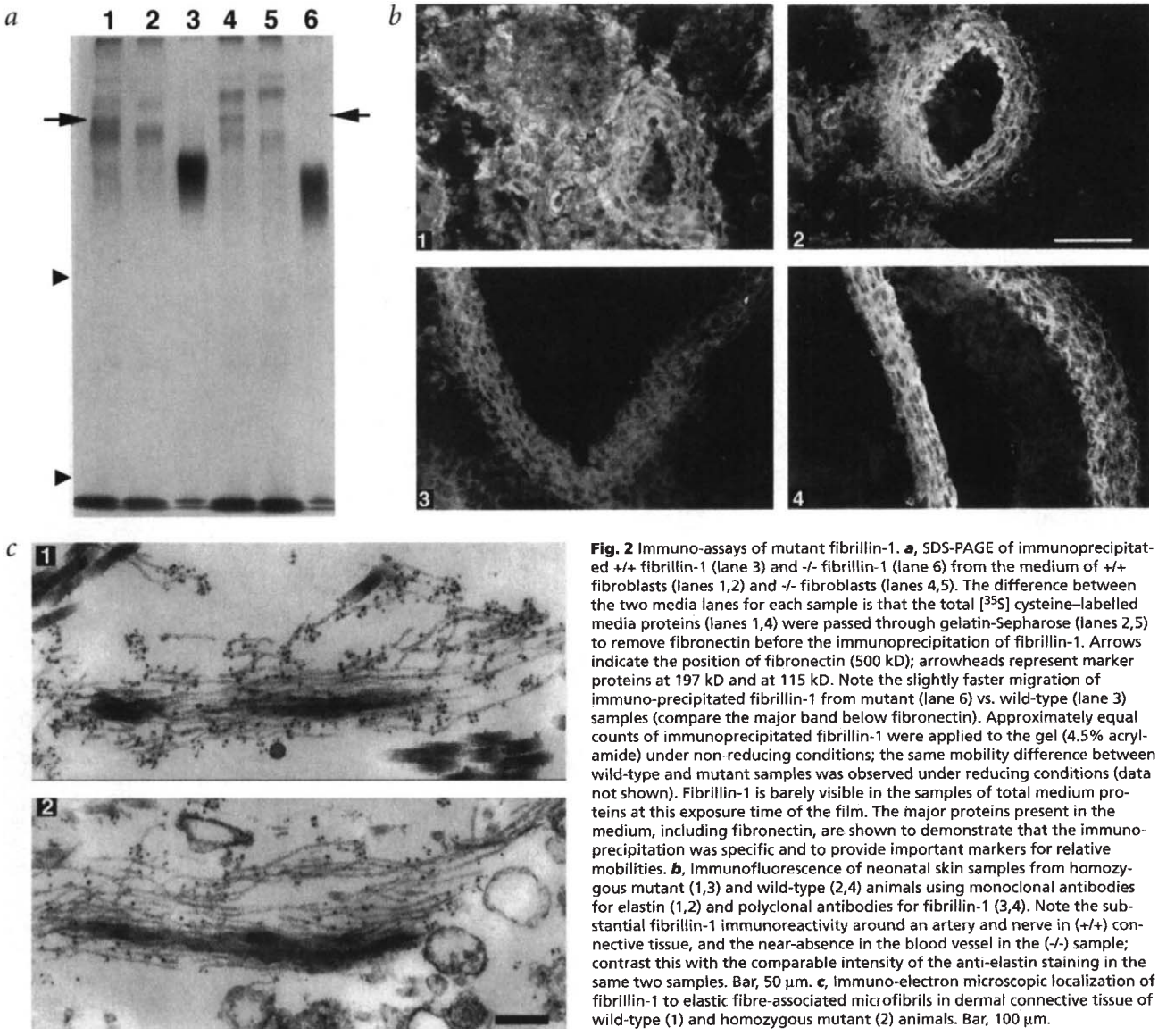

Fig. 2 Immuno-assays of mutant fibrillin-1. ***a***, SDS-PAGE of immunoprecipitated +/+ fibrillin-1 (lane 3) and -/- fibrillin-1 (lane 6) from the medium of +/+ fibroblasts (lanes 1,2) and -/- fibroblasts (lanes 4,5). The difference between the two media lanes for each sample is that the total [^{35}S] cysteine–labelled media proteins (lanes 1,4) were passed through gelatin-Sepharose (lanes 2,5) to remove fibronectin before the immunoprecipitation of fibrillin-1. Arrows indicate the position of fibronectin (500 kD); arrowheads represent marker proteins at 197 kD and at 115 kD. Note the slightly faster migration of immuno-precipitated fibrillin-1 from mutant (lane 6) vs. wild-type (lane 3) samples (compare the major band below fibronectin). Approximately equal counts of immunoprecipitated fibrillin-1 were applied to the gel (4.5% acrylamide) under non-reducing conditions; the same mobility difference between wild-type and mutant samples was observed under reducing conditions (data not shown). Fibrillin-1 is barely visible in the samples of total medium proteins at this exposure time of the film. The major proteins present in the medium, including fibronectin, are shown to demonstrate that the immunoprecipitation was specific and to provide important markers for relative mobilities. ***b***, Immunofluorescence of neonatal skin samples from homozygous mutant (1,3) and wild-type (2,4) animals using monoclonal antibodies for elastin (1,2) and polyclonal antibodies for fibrillin-1 (3,4). Note the substantial fibrillin-1 immunoreactivity around an artery and nerve in (+/+) connective tissue, and the near-absence in the blood vessel in the (-/-) sample; contrast this with the comparable intensity of the anti-elastin staining in the same two samples. Bar, 50 µm. ***c***, Immuno-electron microscopic localization of fibrillin-1 to elastic fibre-associated microfibrils in dermal connective tissue of wild-type (1) and homozygous mutant (2) animals. Bar, 100 µm.

Collectively, the analyses indicate that lack of normal fibrillin-1 is compatible with the development of a viable embryo, and with the maturation of histologically normal elastic matrices. The current model of MFS pathogenesis requires high levels of abnormal fibrillin-1, with dominant negative activity[1,2]. Patients heterozygous for nonsense *FBN1* alleles that are associated with low levels of mutant transcripts can exhibit mild disease phenotype and show preserved matrix deposition of proteins derived from the wild-type allele. In contrast, patients expressing high levels of mutant proteins fail to efficiently utilize wild-type proteins, resulting in a sparse and disorganized network of microfibrils. Thus, despite the complex nature of the *mg*Δ mutation, the resulting biochemical, cellular and clinical phenotypes remain highly relevant to the human condition. The lack of skeletal manifestations in mutant homozygotes implies either species-specific physiological differences or a distinct pathogenesis requiring a mutant product with gain-of-function effects for the development of skeletal manifestations. Alternatively, the mice may simply die before overt expression of skeletal abnormalities.

Correlative evidence implicated fibrillin-1 in regulating elastogenesis[4]. By contrast, our findings support the alternative hypothesis that fibrillin-1 is predominantly involved in tissue homeostasis[12]. They also demonstrate that the length of the polypeptide is not a critical determinant of fibrillin-1 polymerization. It remains to be determined whether the resulting microfibrils are functionally competent and protective of tissues that are not exposed to severe tensile stresses. Because the advential layer is thought to sustain the bulk of haemodynamic stress[15], we propose that aortic dilation in MFS results primarily from loss of tensile strength by the adventitia, in which fibrillin-1 microfibrils may be required to properly organize the primarily collagenous connective tissue. This mechanical collapse, in turn, leads to overstretching and fracturing of the elastic laminae of the media, a process that is facilitated by the failure of fibrillin-1 microfibrils to weave the elastic lamellae in the media and to anchor the endothelial layer of the intima[16]. This new model of vascular pathogenesis in MFS is consistent with the absence of aortic dilation and dissection in patients with mutations of fibrillin-2 or elastin, which would be expected to manifest primarily in the tunica media rather than the adventitia[17,18]. In this light, therapeutic interventions aimed at reducing haemodynamic stress or correcting the basic defect in MFS may have the opportunity to rescue a vessel wall with relatively preserved structure and function.

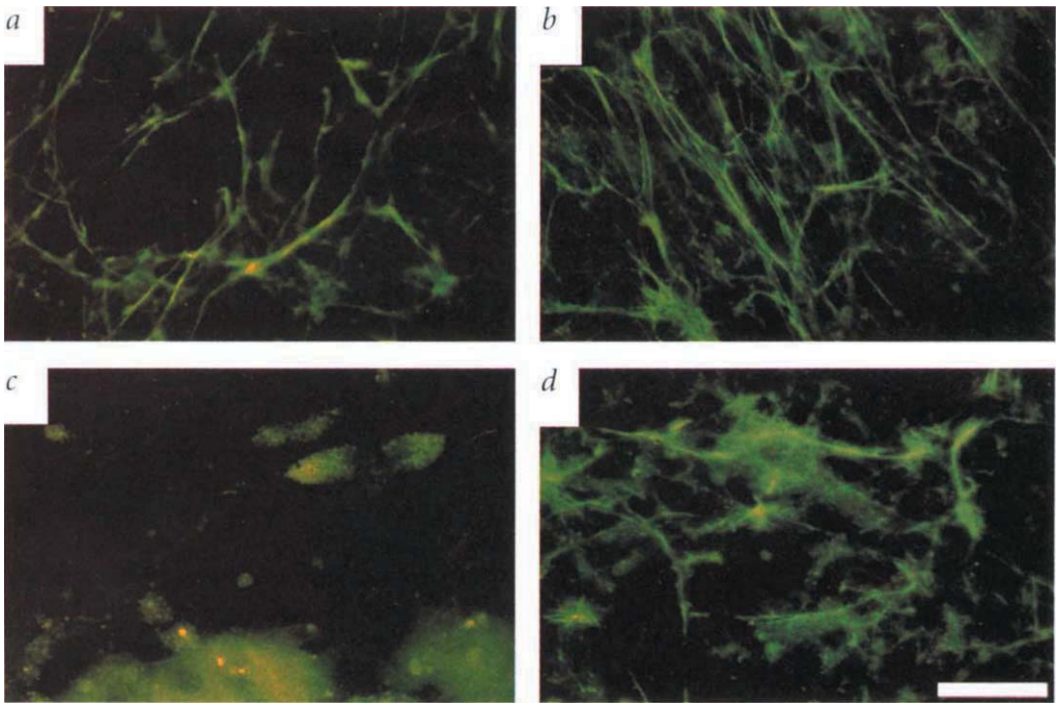

Fig. 3 Fibrillin-1 deposition in cell cultures. Immuno-fluorescence of cultured dermal fibroblasts from wild-type (***a,b***) and homozygous mutant (***c,d***) neonates by fibrillin 1 antisera; cells were processed 72 and 120 hours after plating (1,3 and 2,4). Bar, 50 μm.

Methods

Gene targeting and RNA evaluation. Generation of positively targeted embryonic stem-cell clones and production of chimaeric mice were performed as previously described[19,20]. The analyses described in this study were performed on the progeny of the first three *mgΔ* intercrosses. Survival of homozygous mutant mice was followed for 30 animals that had died within one to eighteen days, and mostly (thirteen animals) at nine or ten days, after birth. Relative RNA levels were estimated from skin samples pooled from five newborn animals by quantitative scanning of northern and slot-blot hybridizations using the NIH-image software[21]. Competitive RT-PCR[22] was performed with RNA from lung, skin and skeletal muscle of two randomly chosen animals. After a linear relationship had been established between input RNA and RT-PCR product, 5 μg of total RNA was reverse transcribed and aliquots were amplified for 25 cycles (annealing at 55 °C; amplification cycle, 94 °C×1′, 55 °C×1′ and 72 °C×1′) in the presence of decreasing amounts of competitor molecules. Samples were normalized

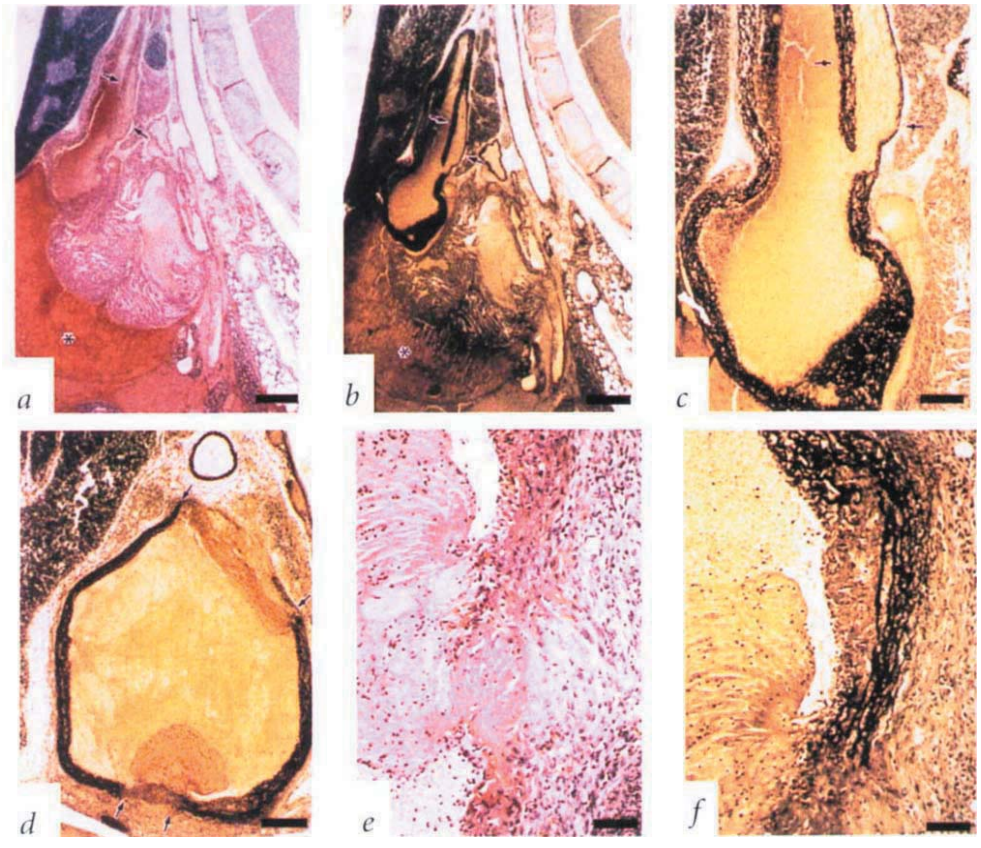

Fig. 4 Histomorphology of mutant vasculature. Homozygous mutant mice (***a,b,c***) with aortic dissection (arrows), haemopericardium (*) and haemothorax. Haematoxylin and eosin (1); Verhoeff–van Gieson (*b,c*). Bar, 800 μm (*a,b*); bar, 260 μm (*c*). Homozygous mutant mice (***d,e,f***) with thrombosis of the aortic wall (*d*, arrows), disruption of the elastic fibres and proliferation of adventitial cells (*e,f*). Haematoxylin and eosin (*d*); Verhoeff–van Gieson (*e,f*). Bar, 320 μm (*d*); bar, 80 μm (*e,f*).

against GAPD levels also measured by competitive RT-PCR. The *Fbn1* competitor contains additional 95 bp, whereas the GAPD plasmid lacks 88 bp. Equilibrium in the concentration between endogenous and exogenous products was determined by scanning ethidium-stained agarose gels.

Immunoassays. Polyclonal antibodies were generated against the recombinant peptide (rF11) that encompasses the amino-terminal half of fibrillin-1 (ref. 23). Immunoblotting experiments showed no detectable cross-reactivity with rF37 (ref. 24), an amino-terminal recombinant peptide of fibrillin-2 (data not shown). The mouse monoclonal antibody specific for elastin has been described[25]. Tissues were derived from newborn mice and wild-type littermates, and cells were established from skin explants. For cell cultures, approximately 2×10^5 fibroblasts were plated onto 1-ml glass chamber slides. All immuno-assays were performed according to published protocols[3,26,27].

Histological analysis. Mice were fixed by immersion in Bouin's fluid, sectioned sagittally in three or four planes and routinely processed for paraffin embedding[8]. Five-micron sections were stained with haematoxylin and eosin, and adjacent serial sections were stained with Verhoeff–van Gieson stain for elastic tissue.

Acknowledgements

We thank J. Bonadio, P. Greenwel, R. Jaenisch, K. Kelley, T. Lufkin, H. Stuhlman and H. Zhang for helpful discussions and suggestions; N. Charbonneau, V. Mohan and C. Ridgway for excellent technical assistance; R. Valentino for inspiring the study; and K. Frith for preparing the manuscript. This work was supported by grants from the NIH (AR42044, AR41135), Shriners Hospital, Howard Hughes Medical Institute, National Marfan Foundation, Dana and Albert Broccoli Center for Aortic Diseases, Smilow Foundation and Dr. Amy and James Elster Research Fund.

Received 13 February; accepted 21 July 1997.

1. Dietz, H., Ramirez, F. & Sakai, L. Marfan syndrome and other microfibrillar diseases. in *Advances in Human Genetics,* vol. 22 (eds Harris, H. & Hirschhorn, K.) 153–186 (Plenum, New York, 1994).
2. Dietz, H. & Pyeritz, R. Mutations in the human gene for fibrillin-1 (*FBN1*) in the Marfan syndrome and related disorders. *Hum. Mol. Genet.* **4**, 1799–1809 (1995).
3. Sakai, L., Keene, D.R. & Engvall, E. Fibrillin, a new 350-kD glycoprotein, is a component of extracellular microfibrils. *J. Cell Biol.* **103**, 2499–2509 (1986).
4. Mecham, R.P. & Davis, E. Elastic fiber structure and assembly. in *Extracellular Matrix Assembly and Structure* (eds Yurchenco, P.D., Birk, D.E. & Mecham, R.P.) 281–314 (Academic Press, New York, 1994).
5. Pereira, L *et al.* Genomic organization of the sequence coding for fibrillin, the defective gene product in Marfan syndrome. *Hum. Mol. Genet.* **2**, 961–968 (1993).
6. Kainulainen, K., Karttunen, L., Puhakka, L., Sakai, L. & Peltonen L. Mutations in the fibrillin gene responsible for dominant ectopia lentis and neonatal Marfan syndrome. *Nature Genet.* **6**, 64–69 (1994).
7. Ramirez, F. Fibrillin mutations in Marfan syndrome and related phenotypes. *Curr. Opin. Genet. Dev.* **6**, 309–315 (1996).
8. Hogan, B., Beddington, R., Constantini, F. & Lacy, E. *Manipulating the Mouse Embryo: A Laboratory Manual,* 2nd ed. (Cold Spring Harbor Laboratory, Cold Spring Harbor, New York, 1994).
9. Zhang, H. *et al.* Structure and expression of fibrillin-2, a novel microfibrillar component preferentially located in elastic matrices. *J. Cell Biol.* **124**, 855–863 (1994).
10. Fiering, S. *et al.* Targeted deletion of 5′ HS2 of the murine b-globin LCR reveals that it is not essential for proper regulation of the b-globin locus. *Genes Dev.* **9**, 2203–2213 (1995).
11. Pham, C.T.N., MacIvor, D.M., Hug, B.A., Heusel, J.W. & Ley, T.J. Long-range disruption of gene expression by a selectable marker cassette. *Proc. Natl. Acad. Sci. USA* **93**, 13090–13095 (1996).
12. Zhang, H., Hu, W. & Ramirez, F. Developmental expression of fibrillin genes suggests heterogeneity of extracellular microfibrils. *J. Cell Biol.* **123**, 1165–1176 (1995).
13. Davis, E.C. Smooth muscle cell to elastic lamina connections in developing mouse aorta: role in aortic medial organization. *Lab. Invest.* **68**, 89–97 (1993).
14. Hollister, D.W., Godfrey, M., Sakai, L.Y. & Pyeritz, R.E. Marfan syndrome: immunohistologic abnormalities of the microfibrillar fiber system. *N. Engl. J. Med.* **323**, 935–939 (1990).
15. Tilson D.M., Elefteriades J. & Brophy C.M. Tensile strength and collagen in abdominal aortic aneurysm disease. in *The Cause and Management of Aneurysms* (eds Greenhalgh, M. & Mannick, J.A.) 97–104 (Latimer Trend, Plymouth UK, 1990).
16. Davis, E.C. Immunolocalization of microfibril and microfibril-associated proteins in the subendothelial matrix of the developing mouse aorta. *J. Cell Sci.* **107**, 727–736 (1994).
17. Putnam, E.A, Zhang, H., Ramirez, F. & Milewicz, D.M. Fibrillin-2 (*FBN2*) mutations result in the Marfan-like disorder, congenital contractural arachnodactyly. *Nature Genet.* **11**, 456–458 (1995).
18. Ewart, A.K., Jin, W., Atkinson, D.L., Morris, C.A. & Keating M.T. Supravalvular aortic stenosis associated with a deletion disrupting the elastin gene. *J. Clin. Invest.* **93**, 1071–1077 (1994).
19. Li, E., Bestor, T.H. & Jaenisch, R. Targeted mutation of the DNA methyltransferase gene results in embryonic lethality. *Cell* **63**, 915–926 (1992).
20. Andrikopoulos, K., Liu, X., Keene, R.D., Jaenisch, R. & Ramirez, F. Targeted mutation in the *col5a2* gene reveals a regulatory role for type V collagen during matrix assembly. *Nature Genet.* **9**, 31–36 (1995).
21. Sambrook, E., Fritsch, E.F. & Maniatis, T. *Molecular Cloning: A Laboratory Manual* (Cold Spring Harbor Laboratory, Cold Spring Harbor, New York, 1989).
22. Gause, W.C. & Adamovicz, J. Use of PCR to quantitate relative differences in gene expression. in *PCR Primer: A Laboratory Manual* (eds Dieffenbach, C.W. & Dveksler, G.S.) 293–338 (Cold Spring Harbor Laboratory, Cold Spring Harbor, New York, 1989).
23. Reinhardt, D.P. *et al.* Fibrillin 1: organization in microfibrils and structural properties. *J. Mol. Biol.* **258**, 104–115 (1996).
24. Keene, D.R. *et al.* Fibrillin-1 in human cartilage: developmental expression and formation of special banded fibrils. *J. Histochem. Cytochem.* (in the press).
25. Hurle, J.M. *et al.* Elastin exhibits a distinctive temporal and spatial pattern of distribution in the developing chick limb in association with the establishment of the cartilaginous skeleton *J. Cell Sci.* **107**, 2623–2634 (1994).
26. Sakai, L.Y., Keene, D.R., Glanville, R.A. & Bächinger, H.P. Purification and partial characterization of fibrillin, a cystine-rich structural component of connective tissue microfibrils. *J. Biol. Chem.* **266**, 14763–14770 (1991).
27. Sakai, L.Y. & Keene, D.R. Fibrillin: monomers and microfibrils. *Methods Enzymol.* **245**, 29–52 (1994).